

# 1 Depth-First Search in Directed Graphs, Revisited

2 **Eric Allender** 

3 Rutgers University, USA

4 <http://www.cs.rutgers.edu/~allender>

5 [allender@cs.rutgers.edu](mailto:allender@cs.rutgers.edu)

6 **Archit Chauhan**

7 Chennai Mathematical Institute, India

8 <https://www.cmi.ac.in/people/fac-profile.php?id=archit>

9 [archit.chauhan@gmail.com](mailto:archit.chauhan@gmail.com)

10 **Samir Datta**

11 Chennai Mathematical Institute, India

12 <https://www.cmi.ac.in/~sdatta/>

13 [sdatta@cmi.ac.in](mailto:sdatta@cmi.ac.in)

## 14 — Abstract —

15 We present an algorithm for constructing a depth-first search tree in planar digraphs; the algorithm  
 16 can be implemented in the complexity class UL, which is contained in nondeterministic logspace  
 17 NL, which in turn lies in  $\text{NC}^2$ . Prior to this (for more than a quarter-century), the fastest uniform  
 18 deterministic parallel algorithm for this problem was  $O(\log^{10} n)$  (corresponding to the complexity  
 19 class  $\text{AC}^{10} \subseteq \text{NC}^{11}$ ).

20 We also consider the problem of computing depth-first search trees in other classes of graphs,  
 21 and obtain additional new upper bounds.

22 **2012 ACM Subject Classification** Complexity Classes, Parallel Algorithms

23 **Keywords and phrases** Depth-First Search, Planar Digraphs, Parallel Algorithms, Space-Bounded  
 24 Complexity Classes

25 **Funding** *Eric Allender*: Supported in part by NSF Grant CCF-1909216.

26 *Archit Chauhan*: Partially supported by a grant from Infosys foundation and TCS PhD fellowship.

27 *Samir Datta*: Partially supported by a grant from Infosys foundation and SERB-MATRICS grant  
 28 MTR/2017/000480.

## 29 **1** Introduction

30 Depth-first search trees (DFS trees) constitute one of the most useful items in the algorithm  
 31 designer's toolkit, and for this reason they are a standard part of the undergraduate al-  
 32 gorithmic curriculum around the world. When attention shifted to parallel algorithms in  
 33 the 1980's, the question arose of whether NC algorithms for DFS trees exist. An early  
 34 negative result was that the problem of constructing the *lexicographically least* DFS tree  
 35 in a given digraph is complete for P [19]. But soon thereafter significant advances were  
 36 made in developing parallel algorithms for DFS trees, culminating in the  $\text{RNC}^7$  algorithm of  
 37 Aggarwal, Anderson, and Kao [1]. This remains the fastest parallel algorithm for the problem  
 38 of constructing DFS trees in general graphs, in the probabilistic setting, or in the setting of  
 39 nonuniform circuit complexity. It remains unknown if this problem lies in (deterministic) NC  
 40 (and we do not solve that problem here).

41 More is known for various restricted classes of graphs. For directed acyclic graphs (DAGs),  
 42 the lexicographically-least DFS tree from a given vertex can be computed in  $\text{AC}^1$  [9]. (See  
 43 also [10, 7, 12, 18, 15, 14].) For undirected planar graphs, an  $\text{AC}^1$  algorithm for DFS trees  
 44 was presented by Hagerup [13]. For more general planar directed graphs Kao and Klein  
 45 presented an  $\text{AC}^{10}$  algorithm. Kao subsequently presented an  $\text{AC}^5$  algorithm for DFS in

46 *strongly connected* planar digraphs. In stating the complexity results for this prior work  
 47 in terms of complexity classes (such as  $AC^1$ ,  $AC^{10}$ , etc.), we are ignoring an aspect of this  
 48 earlier work that was of particular interest to the authors of this earlier work: minimizing  
 49 the number of processors. This is because our focus is on classifying the complexity of  
 50 constructing DFS trees in terms of complexity classes. Thus, if we reduce the complexity  
 51 of a problem from  $AC^{10}$  to  $NC^2$ , then we view this as a significant advance, even if the  $NC^2$   
 52 algorithm uses many more processors (so long as the number of processors remains bounded  
 53 by a polynomial). Indeed, our algorithms rely on the logspace algorithm for undirected  
 54 reachability [20], which does not directly translate into a processor-efficient algorithm. We  
 55 suspect that our approach can be modified to yield a more processor-efficient  $AC^1$  algorithm,  
 56 but we leave that for others to investigate.

## 57 1.1 Our Contributions

58 First, we observe that, given a DAG  $G$ , computation of a DFS tree in  $G$  logspace reduces to  
 59 the problem of reachability in  $G$ . Thus, for general DAGs, computation of a DFS tree lies in  
 60 NL, and for planar DAGs, the problem lies in  $UL \cap \text{co-UL}$  [8, 22]. For classes of graphs where  
 61 the reachability problem lies in L, so does the computation of DFS trees. One such class  
 62 of graphs is planar DAGs with a single source (see [2], where this class of graphs is called  
 63 SMPDs, for **S**ingle-source, **M**ultiple-sink, **P**lanar **D**AGs).

64 For undirected planar graphs, it was shown in [3] that the approach of Hagerup's  $AC^1$   
 65 DFS algorithm [13] can be adapted in order to show that construction of a DFS tree in a  
 66 planar *undirected* graph logspace-reduces to computing the distance between two nodes in  
 67 a planar digraph. Since this latter problem lies in  $UL \cap \text{co-UL}$  [23], so does the problem of  
 68 DFS for planar *undirected* graphs.

69 Our main contribution in the current paper is to show that a more sophisticated application  
 70 of the ideas in [13] lead to a  $UL \cap \text{co-UL}$  algorithm for construction of DFS trees in planar  
 71 *directed* graphs. Since  $UL \subseteq NL \subseteq AC^1 \subseteq NC^2$ , this is a significant improvement over the best  
 72 previous parallel algorithm for this problem: the  $AC^{10}$  algorithm of [17], which has stood for  
 73 27 years.

## 74 2 Preliminaries

75 We assume that the reader is familiar with depth-first search trees (DFS trees).

76 We further assume that the reader is familiar with the standard complexity classes L, NL  
 77 and P (see e.g. the text [6]). We will also make frequent reference to the logspace-uniform  
 78 circuit complexity classes  $NC^k$  and  $AC^k$ .  $NC^k$  is the class of problems for which there is  
 79 a logspace-uniform family of circuits  $\{C_n\}$  consisting AND, OR, and NOT gates, where  
 80 the AND and OR gates have fan-in two and each circuit  $C_n$  has depth  $O(\log^k n)$ . (The  
 81 logspace-uniformity condition implies that each  $C_n$  has only  $n^{O(1)}$  gates.)  $AC^k$  is defined  
 82 similarly, although the AND and OR gates are allowed unbounded fan-in. An equivalent  
 83 characterization of  $AC^k$  is in terms of concurrent-read concurrent-write PRAMs with running  
 84 time  $O(\log^k n)$ . For more background on these circuit complexity classes, see, e.g., the text  
 85 [24].

86 A nondeterministic Turing machine is said to be *unambiguous* if, on every input  $x$ , there is  
 87 at most one accepting computation path. If we consider logspace-bounded nondeterministic  
 88 Turing machines, then unambiguous machines yield the class UL. A set  $A$  is in  $\text{co-UL}$  if and  
 89 only if its complement lies in UL.

The construction of DFS trees is most naturally viewed as a *function* that takes a graph  $G$  and a vertex  $v$  as input, and produces as output an encoding of a DFS tree in  $G$  rooted at  $v$ . But the complexity classes mentioned above are all defined as sets of *languages*, instead of as sets of *functions*. Since our goal is to place DFS tree construction into the appropriate complexity classes, it is necessary to discuss how the complexity of functions fits into the framework of complexity classes.

When  $\mathcal{C}$  is one of  $\{\mathbf{L}, \mathbf{P}\}$ , it is fairly obvious what is meant by “ $f$  is computable in  $\mathcal{C}$ ”; the classes of logspace-computable functions and polynomial-time-computable functions should be familiar to the reader. However, the reader might be less clear as to what is meant by “ $f$  is computable in  $\mathbf{NL}$ ”. As it turns out, essentially all of the reasonable possibilities are equivalent. Let us denote by  $\mathbf{FNL}$  the class of functions that are computable in  $\mathbf{NL}$ ; it is shown in [16] each of the three following conditions is equivalent to “ $f \in \mathbf{FNL}$ ”.

1.  $f$  is computed by a logspace machine with an oracle from  $\mathbf{NL}$ .
2.  $f$  is computed by a logspace-uniform  $\mathbf{NC}^1$  circuit family with oracle gates for a language in  $\mathbf{NL}$ .
3.  $f(x)$  has length bounded by a polynomial in  $|x|$ , and the set  $\{(x, i, b) : \text{the } i^{\text{th}} \text{ bit of } f(x) \text{ is } b\}$  is in  $\mathbf{NL}$ .

Rather than use the unfamiliar notation “ $\mathbf{FNL}$ ”, we will abuse notation slightly and refer to certain functions as being “computable in  $\mathbf{NL}$ ”.

The proof of the equivalence above relies on the fact that  $\mathbf{NL}$  is closed under complement. Thus it is far less clear what it should mean to say that a function is “computable in  $\mathbf{UL}$ ” since it remains an open question if  $\mathbf{UL}$  is closed under complement (although it is widely conjectured that  $\mathbf{UL} = \mathbf{NL}$ ) [21, 5]). However the proof from [16] carries over immediately to the class  $\mathbf{UL} \cap \mathbf{co-UL}$ . That is, the following conditions are equivalent:

1.  $f$  is computed by a logspace machine with an oracle from  $\mathbf{UL} \cap \mathbf{co-UL}$ .
2.  $f$  is computed by a logspace-uniform  $\mathbf{NC}^1$  circuit family with oracle gates for a language in  $\mathbf{UL} \cap \mathbf{co-UL}$ .
3.  $f(x)$  has length bounded by a polynomial in  $|x|$ , and the set  $\{(x, i, b) : \text{the } i^{\text{th}} \text{ bit of } f(x) \text{ is } b\}$  is in  $\mathbf{UL} \cap \mathbf{co-UL}$ .

Thus, if any of those conditions hold, we will say that “ $f$  is computable in  $\mathbf{UL} \cap \mathbf{co-UL}$ ”.

The important fact that the composition of two logspace-computable functions is also logspace-computable (see, e.g., [6]) carries over with an identical proof to the functions computable in  $\mathbf{L}^C$  for any oracle  $C$ . Thus the class of functions computable in  $\mathbf{UL} \cap \mathbf{co-UL}$  is also closed under composition. We make implicit use of this fact frequently when presenting our algorithms. For example, we may say that a colored labeling of a graph  $G$  is computable in  $\mathbf{UL} \cap \mathbf{co-UL}$ , and that, given such a colored labeling, a decomposition of the graph into layers is also computable in logspace, and furthermore, that – given such a decomposition of  $G$  into layers – an additional coloring of the smaller graphs is computable in  $\mathbf{UL} \cap \mathbf{co-UL}$ , etc. The reader need not worry that a logspace-bounded machine does not have adequate space to store these intermediate representations; the fact that the final result is also computable in  $\mathbf{UL} \cap \mathbf{co-UL}$  follows from closure under composition. In effect, the bits of these intermediate representations are re-computed each time we need to refer to them.

### 3 DFS in DAGs logspace reduces to Reachability

In this section, we observe that constructing the lexicographically-least DFS tree in a DAG  $G$  can be done in logspace given an oracle for reachability in  $G$ . But first, let us define what we mean by the lexicographically-first DFS tree in  $G$ :

## 4 Depth-First Search in Directed Graphs, Revisited

136 ► **Definition 1.** Let  $G$  be a DAG, with the neighbours of the vertices given in some order  
 137 in the input. (For example, with adjacency lists, we can consider the ordering in which the  
 138 neighbors are presented in the list). Then the lexicographic first DFS traversal of  $G$  is the  
 traversal done by the following procedure:

```

Input:  $(G, v)$ 
Output: Sequence of edges in DFS tree
visited[ $v$ ]  $\leftarrow$  1
for every out neighbour  $w$  of  $v$ , in the given order do
  | if visited[ $w$ ] = 0 then
  | |   print( $v, w$ )
  | |   DFS( $G, w$ )
  | end
end

```

■ **Algorithm 1** Static DFS routine

139

140 That is, the lexicographically-first DFS tree is merely a DFS tree, but with the (very  
 141 natural) condition that the children of every vertex are explored in the order given in the  
 142 input.

143 When we apply this procedure as part of our algorithm for DFS in planar graphs, we will  
 144 need to to apply it to directed acyclic *multigraphs* (i.e., graphs with parallel edges between  
 145 vertices) where there is a logspace-computable function  $f(v, e)$  that computes the ordering  
 146 of the neighbors of vertex  $v$ , assuming that  $v$  is entered using edge  $e$ . (That is, if the DFS  
 147 tree visits vertex  $v$  from vertex  $x$ , and there are several parallel edges from  $x$  to  $v$ , then the  
 148 ordering of the neighbors of  $v$  may be different, depending on which edge is followed from  $x$   
 149 to  $v$ .)

150 As is observed in [9], the unique path from  $s$  to another vertex  $v$  in the lexicographically-  
 151 least DFS tree in  $G$  rooted at  $s$  is the lexicographically-least path in  $G$  from  $s$  to  $t$ .

152 Now consider the following simple algorithm for constructing the lexicographically-least  
 153 path in a DAG  $G$  from  $s$  to  $v$ , where:

```

Input:  $(G, s, v, f)$ 
Output: Lex least path from  $s$  to  $v$  under  $f$ 
current  $\leftarrow$   $s$ ;  $e \leftarrow$  null;
while (current  $\neq$   $v$ ) do
  | child  $\leftarrow$  first child of current (in the order given by  $f(\text{current}, e)$ )
  | while (REACH(child,  $v$ )  $\neq$  TRUE) do
  | | child  $\leftarrow$  next child of current (in the order given by  $f(\text{current}, e)$ )
  | end
  |  $e \leftarrow$  (current, child); current = child;
end

```

■ **Algorithm 2** DAG DFS routine

154 The correctness of this algorithm is essentially shown by the proof of Theorem 11 of [9].

155 The algorithm for computing the lexicographically-least DFS tree rooted at  $s$  can thus be  
 156 presented as the composition of two functions  $g$  and  $h$ , where  $g(G, s) = (G, s, L)$ , where  $L$  is  
 157 a list of all of the lexicographically-least paths from  $s$  to each vertex  $v$ . Note that the set of  
 158 edges in the DFS tree in  $G$  rooted at  $s$  is exactly the set of edges that occur in the list  $L$

159 in  $g(G, s) = (G, s, L)$ . Then  $h(G, s, L)$  is just the result of removing from  $G$  each edge that  
 160 does not appear in  $L$ . The function  $h$  is computable in logspace, whereas  $g$  is computable in  
 161 logspace with an oracle for reachability in  $G$ .

162 Since reachability in DAGs is a canonical complete problem for NL, we obtain the following  
 163 corollary:

164 ► **Corollary 2.** *Construction of lexicographically-first DFS trees for DAGs lies in NL.*

165 Similarly, since reachability in planar directed (not-necessarily acyclic) graphs lies in  
 166  $UL \cap \text{co-UL}$  [8, 22], we obtain:

167 ► **Corollary 3.** *Construction of lexicographically-first DFS trees for planar DAGs lies in*  
 168  $UL \cap \text{co-UL}$ .

169 A DAG  $G$  is said to be a SMPD if it contains at most one vertex of indegree zero.  
 170 Reachability in SMPDs is known to lie in L [2].

171 ► **Corollary 4.** *Construction of lexicographically-first DFS trees for SMPDs lies in L.*

### 172 3.1 DFS in a planar digraph with a single cycle

173 We now consider a special case that will form a useful subroutine for us: graphs in which  
 174 there is a single cycle, forming the external face of the embedding. That is, let  $G$  be a  
 175 planar digraph such that the external face is a directed cycle  $C$  and  $G - V(C)$  is a DAG  
 176 (or, alternatively, a directed acyclic *multigraph*). Then we can do DFS in  $G$  starting from  
 177 an arbitrary vertex in  $C$  in  $UL \cap \text{co-UL}$ . The DFS completes the cycle first and then, while  
 178 backtracking, performs DFS in the reachable but as yet untraversed part of the digraph.

179 We now provide more details: Let the vertices in the directed cycle  $C$  be  $v_0, \dots, v_k$ ,  
 180 in this order, where the entry point in the cycle is  $v_0$ . Let  $R(v_i) \subseteq V(G) \setminus V(C)$  be  
 181 the set of vertices reachable from  $v_i$  in the graph excluding the cycle. We let  $R'(v_i) =$   
 182  $R(v_i) \setminus \bigcup_{j=i+1}^k R(v_j)$ .

183 A logspace routine with an oracle for the  $UL \cap \text{co-UL}$  problem of reachability in planar  
 184 graphs can construct each of the sets  $R'(v_i)$ . It is clear that each  $R'(v_i)$  induces a DAG  
 185 which (if non-empty) consists of vertices reachable from  $v_i$  but not from subsequent  $v_j$ 's.  
 186 Moreover, the  $R'(v_i)$ 's are all pairwise disjoint. Thus a DFS of  $G$  can be performed by doing  
 187 DFS on the graph induced by each  $R'(v_i)$  (using Corollary 3) and unioning with the aforesaid  
 188 DFS of the cycle  $C$ .

189 Note that a graph with a single cycle is a special case of a planar graph in which all  
 190 cycles are clockwise (or all cycles are counterclockwise). By analogy with the *Coriolis effect*,  
 191 we call such graphs *Coriolis graphs*. It turns out that Coriolis graphs play an important role  
 192 in our main algorithm.

## 193 4 Layering the graph

194 The main algorithmic insight that led us to the current algorithm was an approach for finding  
 195 DFS trees in Coriolis graphs. In the exposition below, we first layer the graph in terms of  
 196 clockwise cycles (which we will henceforth call red cycles), and obtain a decomposition of the  
 197 original graph into (essentially) Coriolis graphs. We then apply a nested layering in terms of  
 198 counterclockwise cycles (which we will henceforth call blue cycles); ultimately we decompose  
 199 the graph into units that are structured as a DAG, which we can then process using the  
 200 tools from the earlier sections of the paper. The more detailed presentation follows.

## 201 4.1 Degree Reduction and Expansion

202 ► **Definition 5.** (of  $\mathbf{Exp}^\circ(G)$  and  $\mathbf{Exp}^\circ(G)$ ) Let  $G$  be a planar digraph. The “expanded”  
 203 digraph  $\mathbf{Exp}^\circ(G)$  (respectively,  $\mathbf{Exp}^\circ(G)$ ) is formed by replacing each vertex  $v$  of total degree  
 204  $d(v) > 3$  by a clockwise (respectively, counterclockwise) cycle  $C_v$  on  $d(v)$  vertices such that  
 205 the endpoint of the the  $i$ -th edge incident on  $v$  is now incident on the the  $i$ -th vertex of the  
 206 cycle.

207  $\mathbf{Exp}^\circ(G)$  and  $\mathbf{Exp}^\circ(G)$  each have maximum degree bounded by 3; i.e., they are *subcubic*.  
 208 Next we define the clockwise (and counterclockwise) dual for such a graph and also a notion  
 209 of distance.

210 Recall that for an undirected plane graph  $H$ , the dual (multigraph)  $H^*$  is formed by  
 211 placing, for every edge  $e \in E(H)$ , a dual edge  $e^*$  between the face(s) on either side of  $e$  (see  
 212 Section 4.6 from [11] for more details). Faces  $f$  of  $H$  and the vertices  $f^*$  of  $H^*$  correspond  
 213 to each other as do vertices  $v$  of  $H$  and faces  $v^*$  of  $H^*$ .

214 ► **Definition 6.** (of Duals  $G^\circ$  and  $G^\circ$ ) Let  $G$  be a plane digraph, then the clockwise dual  
 215  $G^\circ$  (respectively, counterclockwise dual  $G^\circ$ ) is a weighted bidirected version of the undirected  
 216 dual of the underlying undirected graph of  $G$  in a way so that the orientation formed by  
 217 rotating the corresponding directed edge of  $G$  in a clockwise (respectively, counterclockwise)  
 218 way gets a weight of 1 and the other orientation gets weight 0. We inherit the definition of  
 219 dual vertices and faces from the underlying undirected dual.

220 ► **Definition 7.** For a plane subcubic digraph  $G$ , let  $f_0$  be the external face. Define the type  
 221  $\mathbf{type}^\circ(f)$  (respectively,  $\mathbf{type}^\circ(f)$ ) of a face to be the singleton set consisting of the distance  
 222 at which  $f$  lies from  $f_0$  in  $G^\circ$ :  $\{d^\circ(f_0, f)\}$  (respectively,  $\{d^\circ(f_0, f)\}$ ). Generalise this to  
 223 edges  $e$  by defining  $\mathbf{type}^\circ(e)$  (respectively  $\mathbf{type}^\circ(e)$ ) as the set consisting of the union of the  
 224  $\mathbf{type}^\circ$  (respectively,  $\mathbf{type}^\circ$ ) of the two faces adjacent to  $e$ , and to vertices  $v$  by defining as  
 225 the  $\mathbf{type}^\circ(v)$  (respectively  $\mathbf{type}^\circ(v)$ ) union of the  $\mathbf{type}^\circ$  (respectively,  $\mathbf{type}^\circ$ ) of the faces  
 226 incident on the vertex  $v$ .

227 The following is a direct consequence of subcubicity and the triangle inequality:

228 ► **Lemma 8.** In every subcubic graph  $G$ , the cardinality  $|\mathbf{type}^\circ(x)|, |\mathbf{type}^\circ(x)|$  where  $x$   
 229 is a face, edge or a vertex is at least one and at most 2 and in the latter case consists of  
 230 consecutive non-negative integers.

231 Further, if  $v \in V(G)$  is such that  $|\mathbf{type}^\circ(v)| = 2$ , then there exist unique  $u, w \in V(G)$ ,  
 232 such that  $(u, v), (v, w) \in E(G)$  and  $|\mathbf{type}^\circ(u, v)| = |\mathbf{type}^\circ(v, w)| = 2$ .

233 We first need a simple lemma:

234 ► **Lemma 9.** Suppose  $(f_1, f_2)$  is a dual edge with weight 1 (and  $(f_2, f_1)$  is of weight 0) then,  
 235  $d^\circ(f_0, f_1) \leq d^\circ(f_0, f_2) \leq d^\circ(f_0, f_1) + 1$ .

236 **Proof.** From the triangle inequality  $d^\circ(f_0, f_1) \leq d^\circ(f_0, f_2) + d^\circ(f_2, f_1) = d^\circ(f_0, f_2)$ . Simil-  
 237 arly,  $d^\circ(f_0, f_2) \leq d^\circ(f_0, f_1) + d^\circ(f_1, f_2) \leq d^\circ(f_0, f_1) + 1$ . ◀

238 **Proof.** (of Lemma 8) Since each vertex  $v \in V(G)$  of a subcubic graph is incident on at most  
 239 3 faces the only case is which  $|\mathbf{type}^\circ(v)| > 2$  corresponds to three distinct faces  $f_1, f_2, f_3$   
 240 being incident on a vertex. But here the undirected dual edges form a triangle such that  
 241 in the directed dual the 1 edges are oriented either as a cycle or acyclically. In the former  
 242 case by three applications of the first half of Lemma 9 we get that  $d^\circ(f_0, f_1) \leq d^\circ(f_0, f_2) \leq$   
 243  $d^\circ(f_0, f_3) \leq d^\circ(f_0, f_1)$ , hence all 3 distances are the same. Therefore  $|\mathbf{type}^\circ(v)| = 1$ .

244 In the latter case, suppose the edges of weight 1 are  $(f_1, f_2), (f_2, f_3), (f_1, f_3)$ , then  
 245 by Lemma 9 we get:  $d^\circ(f_0, f_1) \leq d^\circ(f_0, f_2), d^\circ(f_0, f_3) \leq d^\circ(f_0, f_1) + 1$ . Thus, both  
 246  $d^\circ(f_0, f_2), d^\circ(f_0, f_3)$  are sandwiched between two consecutive values  $d^\circ(f_0, f_1), d^\circ(f_0, f_1) + 1$ .  
 247 Hence  $d^\circ(f_0, f_1), d^\circ(f_0, f_2), d^\circ(f_0, f_3)$  must take at most two distinct values, and thus  
 248  $|\mathbf{type}^\circ(v)| \leq 2$ . Moreover either  $\mathbf{type}^\circ(f_1) \neq \mathbf{type}^\circ(f_2) = \mathbf{type}^\circ(f_3)$  or  $\mathbf{type}^\circ(f_1) =$   
 249  $\mathbf{type}^\circ(f_2) \neq \mathbf{type}^\circ(f_3)$ . Let  $e_1, e_2, e_3$  be such that,  $e_1^\circ = (f_2, f_3), e_2^\circ = (f_1, f_3), e_3^\circ =$   
 250  $(f_1, f_2)$ . Then the two cases correspond to  $|\mathbf{type}^\circ(e_1)| = |\mathbf{type}^\circ(e_2)| = 2, |\mathbf{type}^\circ(e_3)| = 1$   
 251 and to  $|\mathbf{type}^\circ(e_1)| = 1, |\mathbf{type}^\circ(e_2)| = |\mathbf{type}^\circ(e_3)| = 2$  respectively. Noticing that  $e_1, e_3$  are  
 252 both incoming or both outgoing edges of  $v$  completes the proof for the clockwise case. The  
 253 proof for the counterclockwise case is formally identical. ◀

254 ▶ **Definition 10.** For a plane subcubic graph  $G$  as above, we refer to vertices and edges with  
 255 a type of cardinality two in  $G^\circ$  (respectively, in  $G^\circ$ ) as red (respectively, blue) while the  
 256 ones with a cardinality of one as white. The resulting colored graphs are called **red**( $G$ ) and  
 257 **blue**( $G$ ) respectively.

258 We will see later how to apply both the duals in  $G$  to get red and blue layerings of a  
 259 given input graph.

260 Also note that a red (respectively blue) edge must have red (respectively blue) end point  
 261 vertices, as they are adjacent to the same faces as the edge between is.

262 We enumerate some properties of **red**( $G$ ), **blue**( $G$ ) ( $G$  is subcubic):

- 263 ▶ **Lemma 11.** 1. Red vertices and edges in **red**( $G$ ) form disjoint clockwise cycles.  
 264 2. No clockwise cycle in **red**( $G$ ) consists of only white edges (and hence white vertices).  
 265 Similar properties hold for **blue**( $G$ ).

266 **Proof.** 1. Firstly, note that a red edge must have red end point vertices, as they are adjacent  
 267 to the same faces that the edge between them is adjacent to. It is immediate from  
 268 Lemma 8 that if  $v$  is a red vertex, it has exactly one red incoming edge and one red  
 269 outgoing edge, proving this part.

270 2. Suppose  $C$  is a clockwise cycle. Consider the shortest path in  $G^\circ$  from the external face  
 271 to a face enclosed by  $C$ . From the Jordan curve theorem (Theorem 4.1.1 [11]), it must  
 272 cross the cycle  $C$ . The edge dual to the crossing must be red.  
 273 ◀

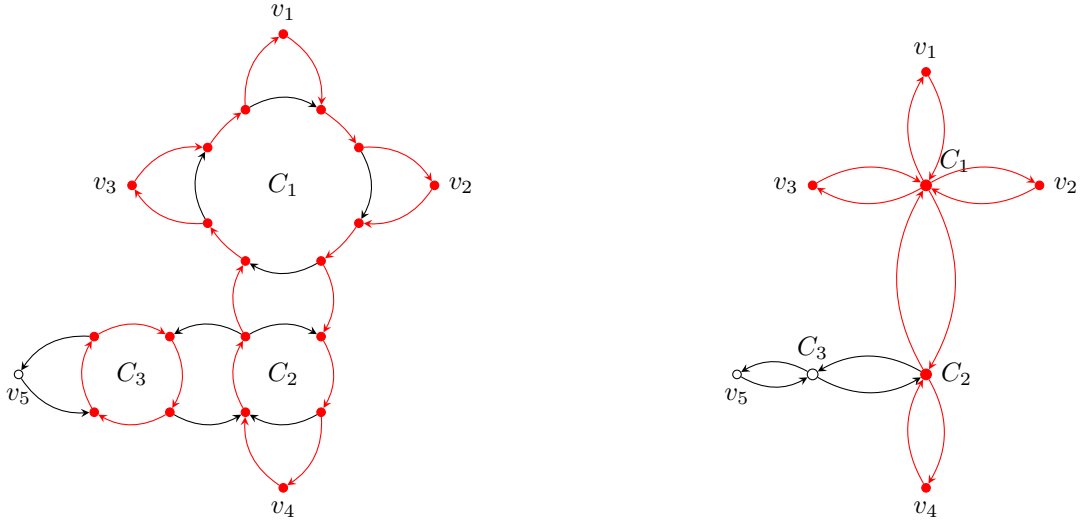
274 The definitions above, which apply only to subcubic plane graphs, can now be extended  
 275 to a general plane graph  $G$ , by considering the subcubic graphs **Exp** $^\circ(G)$  (and **Exp** $^\circ(G)$ ).  
 276 But first, we must make a simple observaion about **red**(**Exp** $^\circ(G)$ ) (and dually about  
 277 **blue**(**Exp** $^\circ(G)$ )).

278 ▶ **Lemma 12.** Let  $v \in V(G)$  be a vertex of degree more than 3. Let  $C_v$  be the corresponding  
 279 expanded cycle in **Exp** $^\circ(G)$ . Suppose at least one edge of  $C_v$  is white in **red**(**Exp** $^\circ(G)$ ) then  
 280 there is a unique red cycle  $C$  that shares edges with  $C_v$ .

281 **Proof.** First we note that  $C_v$  does not contain anything inside it since it is an expanded  
 282 cycle. By lemma 11 we know that  $C_v$  has at least one red edge. Suppose it shares one or  
 283 more edges with a red cycle  $R_1$ . Since both cycles are clockwise and  $C_v$  has nothing inside,  
 284 the cycle  $R_1$  must enclose  $C_v$ . Now suppose there is another red cycle  $R_2$  that shares one or  
 285 more edges with  $C_v$ . Then  $R_2$  must also enclose  $C_v$ . But two cycles cannot enclose a cycle  
 286 whilst sharing edges with it without touching each other, which contradicts the above lemma  
 287 that all red cycles in a subcubic graph are vertex disjoint. ◀

288 The last two lemmas allow us to consistently contract the red cycles in  $\mathbf{red}(\mathbf{Exp}^\circ(G))$ :

289 ► **Definition 13.** The colored graph  $\mathbf{Col}^\circ(G)$  (respectively,  $\mathbf{Col}^\circ(G)$ ) is obtained by labeling  
 290 a degree more than 3 vertex  $v \in V(G)$  as red iff the cycle  $C_v$  in  $\mathbf{red}(\mathbf{Exp}^\circ(G))$  has at least  
 291 one red edge and at least one white edge. Else the color of  $v$  is white. All the low degree  
 292 vertices and edges of  $G$  inherit their colors from  $\mathbf{red}(\mathbf{Exp}^\circ(G))$ . The coloring of  $\mathbf{Col}^\circ(G)$   
 293 is similar.



■ **Figure 1** An example of contracting expanded cycles. The figure on right shows the graph after contracting the expanded cycles  $C_1, C_2, C_3$  according to definition 13

294 We can now characterize the colorings in the graph  $\mathbf{Col}^\circ(G)$ :

295 ► **Lemma 14.** The following hold:

- 296 1. A red cycle in  $\mathbf{Col}^\circ(G)$  is vertex disjoint from every red cycle contained in its interior.
- 297 2. Every 2-connected component of the red subgraph of  $\mathbf{Col}^\circ(G)$  is a simple clockwise cycle.

298 **Proof.** For  $v \in V(G)$ , let  $C_v \subseteq \mathbf{Exp}^\circ(G)$  be the expanded cycle. If it has a red vertex it is  
 299 immediately enclosed by a unique red cycle  $R$  in  $\mathbf{Exp}^\circ(G)$  by Lemma 12. Assuming  $C_v$  is  
 300 not all red, it consists of alternating red subpaths and white subpaths. On contracting  $C_v$  we  
 301 get a collection of clockwise red cycles outside sharing a common cut-vertex  $v$ . Notice that  
 302 the new collection of red cycles consists of edges that  $R$  did not share with  $C_v$ . Also notice  
 303 that (as a thought experiment) if we contracted the  $C_v$ 's that share a vertex with  $R$ , one at  
 304 a time we would get an edge-disjoint set of red cycles with distinct cut vertices. Therefore, in  
 305  $\mathbf{Col}^\circ(G)$ , the red subgraph consists of a collection of connected components, each of which  
 306 is a remnant of exactly one red cycle in  $\mathbf{Exp}^\circ(G)$ ; these connected components consist of  
 307 red cycles that touch externally at cut vertices. Hence both parts of the lemma follow. ◀

308 Although the above lemmas have been proved for the clockwise dual, they also hold for  
 309 counter clockwise dual with red replaced by blue mutatis mutandis.

## 310 4.2 Layering the colored graphs

311 ► **Definition 15.** Let  $x \in V(\mathbf{Col}^\circ(G)) \cup E(\mathbf{Col}^\circ(G))$ . Let  $\ell^\circ(x)$  be one more than the  
 312 minimum integer that occurs in  $\mathbf{type}^\circ(x')$ , for each  $x' \in V(\mathbf{Exp}^\circ(G)) \cup E(\mathbf{Exp}^\circ(G))$  that



313 is contracted to  $x$ . Further let  $\mathcal{L}^k(\mathbf{Col}^\circ(G)) = \{x \in V(\mathbf{Col}^\circ(G)) \cup E(\mathbf{Col}^\circ(G)) : \ell^\circ(x) = k\}$ .  
 314 Similarly define,  $\ell^\circ(x), \mathcal{L}^k(\mathbf{Col}^\circ(G))$ .

315 We call  $\mathcal{L}^k(\mathbf{Col}^\circ(G))$  the  $k^{\text{th}}$  layer of the graph.  
 316 It is easy to see the following from Lemma 14:

317 **► Proposition 16.** For every  $x \in V(\mathbf{Col}^\circ(G)) \cup E(\mathbf{Col}^\circ(G))$  the quantity  $\ell^\circ(x)$  is one more  
 318 than the number of red cycles that strictly enclose  $x$  in  $\mathbf{Col}^\circ(G)$ . All the vertices and edges  
 319 of a red cycle of  $\mathbf{Col}^\circ(G)$  lie in the same layer  $\mathcal{L}^{k+1}(\mathbf{Col}^\circ(G))$  for the enclosure depth  $k$  of  
 320 the cycles.

321 We had already noted above that the red subgraph of  $G$  had simple clockwise cycles as  
 322 its biconnected components. We note a few more lemmas about the structure of a layer of  $G$ :

323 **► Lemma 17.** We have:

- 324 1. A red cycle in a layer  $\mathcal{L}^{k+1}(\mathbf{Col}^\circ(G))$  does not contain any vertex/edge of the same layer  
 325 inside it.
- 326 2. Any clockwise cycle in a layer consists of all red vertices and edges.  
 327 Dually, a blue cycle in a layer does not contain any vertex or edge of the same layer inside it.

328 **► Remark 18.** Notice that the conclusion in the second part of the Lemma fails to hold if we  
 329 allow cycles spanning more than one layer.

330 **Proof.** The first part is a direct consequence of proposition 16. For the second part we mimic  
 331 the proof of the second part of Lemma 11. Consider a clockwise cycle  $C \subseteq \mathcal{L}^{k+1}\mathbf{Col}^\circ G$   
 332 that passes through a white edge  $e$ . Every face adjacent to  $C$  from the outside must have  
 333  $\mathbf{type}^\circ = k$  because  $C$  is contained in layer  $k + 1$ . Then the  $\mathbf{type}^\circ$  of the faces on either  
 334 side of  $e$  is the same and therefore must be  $k$ . Let  $f$  be a face enclosed by  $C$  that has  
 335  $\mathbf{type}^\circ(f) = k$ . Thus it must be adjacent to a face of  $\mathbf{type}^\circ = k - 1$ . But this contradicts  
 336 that every face inside and adjacent to  $C$  must have  $\mathbf{type}^\circ$  at least  $k$ . ◀

337 The above lemmas show that the strongly connected components of the red subgraph of a  
 338 layer consist of red cycles touching each other without nesting, in a tree like structure. This  
 339 prompts the following definition:

340 **► Definition 19.** For a red cycle  $R \subseteq \mathcal{L}^k(\mathbf{Col}^\circ(G))$  we denote by  $G_R$ , the graph induced by  
 341 vertices of  $\mathcal{L}^{k+1}(\mathbf{Col}^\circ(G))$  enclosed by  $R$ .

342 The strongly connected components of the red subgraph of  $G_R$  are called the red clusters  
 343 of  $G_R$ .

344 The cluster graph  $\mathbf{Cl}^\circ(G_R)$  is formed from  $G_R$  by contracting the red clusters of  $G_R$  to  
 345 single nodes along with all the white vertices of  $G_R$  and adding a directed edge between two  
 346 nodes iff there was a directed edge between corresponding vertices in  $G_R$ .

347 We get:

348 **► Lemma 20.** For each red cycle  $R \subseteq \mathcal{L}^k(\mathbf{Col}^\circ(G))$ , the cluster graph  $\mathbf{Cl}^\circ(G_R)$  does not  
 349 contain any clockwise cycle. That is, it is a Coriolis graph.

350 **Proof.** If there is a clockwise cycle  $C \subseteq \mathbf{Cl}^\circ(G_R)$  then there must be a corresponding  
 351 clockwise cycle  $C' \subseteq G_R$  as well. It cannot be all red since otherwise it would map to a  
 352 single vertex in  $\mathbf{Cl}^\circ(G_R)$ . But this contradicts Lemma 17. ◀

353 Next we aim to remove all the counterclockwise cycles in order to construct a DAG in which  
 354 we can do DFS. For this we apply another layering on every layer  $\mathcal{L}^k(\mathbf{Col}^\circ(G))$  of the graph  
 355  $G$  again with the help of Definitions 13, 15, but this time using counterclockwise i.e. blue  
 356 cycles. Thus for every red cycle  $R$  in  $G$ , we consider the graph  $H = \mathbf{Col}^\circ(G_R)$  and its  
 357 layers  $\mathcal{L}^l(H)$  (w.r.t the counterclockwise dual) for non-negative integers  $l$ . Consider a blue  
 358 cycle  $B \subseteq \mathcal{L}^l(H)$  and consider the corresponding blue graph  $H_B$ . By Lemma 20 applied in a  
 359 counterclockwise sense, there is no counterclockwise cycle in the cluster graph  $\mathbf{Cl}^\circ(H_B)$ .

360 The lemmas above about the structure of a red layer also hold for a blue layer with  
 361 suitable changes.

362 It turns out that if we compress the strongly connected components of the colored  
 363 subgraph (both red *and* blue) of a blue layer, we get a DAG.

364 Formally, we start with the combined analog of Definitions 13, 15:

365 ► **Definition 21.** *Each vertex or edge  $x \in V(G) \cup E(G)$  gets a red layer number  $k + 1$  if it  
 366 belongs to  $\mathcal{L}^{k+1}(\mathbf{Col}^\circ(G))$  and a blue layer number  $l + 1$ , if it belongs to  $\mathcal{L}^{l+1}(\mathbf{Col}^\circ(G_R))$   
 367 where  $R \subseteq \mathcal{L}^k(\mathbf{Col}^\circ(G))$  is the red cycle immediately enclosing  $x$ .*

368 *Moreover this defines the colored graph  $\mathbf{Col}(G)$  by giving  $x$  the color red if it is red in  
 369  $\mathbf{Col}^\circ(G)$  and/or blue in  $\mathbf{Col}^\circ(G_R)$  (notice it could be both red and blue) and lastly white if it  
 370 is white in both the graphs. In this case, we say that  $x$  belongs to sublayer  $\mathcal{L}^{k+1,l+1}(\mathbf{Col}(G))$ .*

371 By proposition 16, we can also say that a sublayer  $\mathcal{L}^{k+1,l+1}(\mathbf{Col}(G))$  thus consists of  
 372 edges/vertices that are strictly enclosed inside  $k$  red cycles and inside  $l$  blue cycles that are  
 373 contained *inside* the first enclosing red cycle.

374 We'll see some observations and lemmas regarding the structure of a sublayer now.

375 Since every edge/vertex in  $\mathcal{L}^{k+1,l+1}(\mathbf{Col}(G))$  has the same red AND blue layer number,  
 376 it is clear that there can be no nesting of colored cycles. Also we have:

377 ► **Lemma 22.** *Every clockwise cycle in a sublayer  $\mathcal{L}^{k+1,l+1}(\mathbf{Col}(G))$  consists of all red edges  
 378 and vertices and any every counterclockwise cycle in the sublayer consists of all blue vertices  
 379 and edges. (Some edges/vertices of the cycle can be both red as well as blue)*

380 **Proof.** This is a direct consequence of Lemma 17 applied to the sublayer  $\mathcal{L}^{k+1,l+1}(\mathbf{Col}(G))$ ,  
 381 which is a (counterclockwise) layer in graph  $G_R$  for some red cycle  $R$ . ◀

382 Thus we can refer to clockwise cycles and counterclockwise cycles as red and blue cycles  
 383 respectively.

384 ► **Definition 23.** *For a red or blue colored cycle  $C$  of layer  $\mathcal{L}^{k,l}(\mathbf{Col}(G))$ , we denote by  $G_C$   
 385 the graph induced by vertices of  $\mathcal{L}^{k',l'}(\mathbf{Col}(G))$  enclosed by  $C$ , where  $\{k',l'\}$  is  $\{k+1,1\}$  or  
 386  $\{k,l+1\}$  according to whether  $C$  is red or blue cycle respectively.*

387 Note that two cycles of the same color in  $\mathcal{L}^{k+1,l+1}(G)$  cannot share an edge since neither  
 388 is enclosed by the other – since they belong to the same layer, and they also have the same  
 389 orientation. Cycles of different colors can share edges but we note:

390 ► **Lemma 24.** *Two cycles of a sublayer  $\mathcal{L}^{k+1,l+1}(\mathbf{Col}(G))$  can only share one contiguous  
 391 segment of edges.*

392 **Proof.** Let a red cycle  $R$  and a blue cycle  $B$  in a sublayer share two vertices  
 393  $u, v$  but let the paths  $R(u, v), B(u, v)$  in the two cycles be disjoint. Notice that the graph  
 394  $(R \setminus R(u, v)) \cup B(u, v)$  is also a clockwise cycle that encloses the edges of  $R(u, v)$  contradicting  
 395 the first part of Lemma 17. ◀

396 We consider the strongly connected components of a sublayer and note the following  
397 lemmas regarding them:

398 ► **Lemma 25.** *The strongly connected components of a sublayer, which we call clusters, have  
399 the following properties:*

- 400 1. *Every vertex/edge in them is either blue or red (or possibly both).*
- 401 2. *Every face is a directed cycle (red or blue).*

402 **Proof.** 1. In a strongly connected graph every vertex and edge lies on a cycle and therefore  
403 by Lemma 22 must be colored red or blue (or both).

404 2. Suppose there is a face  $f$  the boundary of which is not a directed cycle. Look at a  
405 directed dual (say clockwise) of the strongly connected component (just the component  
406 independently). This dual must be a DAG since the primal is strongly connected. The  
407 vertex  $f^*$  in the dual corresponding to face  $f$  of the strongly connected component has  
408 in degree at least one and out degree at least one since it has boundary edges of both  
409 orientations. Consider a vertex  $u^*$  of the dual which has an edge  $(u^*, f^*)$  to  $f^*$ . If we  
410 contract this edge, merging  $u^*$  and  $f^*$  to  $f^*$ , the modified dual is still a DAG clearly,  
411 with one less vertex. If we keep merging the vertices incident to  $f^*$  into it, eventually we  
412 must reach a stage when no vertex is incident to  $f^*$ . This merged  $f^*$  is a source since its  
413 in-degree is 0, and hence its outgoing edges form a directed cut for this modified dual.  
414 But this also clearly corresponds to a directed cut in the original dual, with one partition  
415 containing the dual vertex  $f^*$  and all other dual vertices that were merged with  $f^*$ . In  
416 the primal, by cut cycle duality this corresponds to a directed cycle that contains the  
417 face  $f$  and the faces corresponding to the dual vertices merged with  $f^*$ . Thus cycle thus  
418 contains more than one face inside it along with  $f$ , which violates lemma 22 since directed  
419 cycles are empty for that sublayer.

420 ◀

421 The strongly connected components or clusters of a sublayer hence consist of intersecting  
422 red and blue cycles. However they can only intersect in a tree like manner as we will see  
423 from following definition and lemma.

424 We now construct the incidence graph of these strongly connected components. In other  
425 words,

426 ► **Definition 26.** *The nodes of the graph  $\mathbf{S}^{k+1, l+1}(G)$  are the directed cycles of each of  
427 the two colors (viz. red and blue) in the layer  $\mathcal{L}^{k+1, l+1}(\mathbf{Col}(G))$ . Two nodes support an  
428 undirected edge if the corresponding strongly connected components intersect.*

429 We have the following:

430 ► **Lemma 27.**  *$\mathbf{S}^{k+1, l+1}(G)$  is a forest. Given an entry point into a component of  $\mathbf{S}^{k+1, l+1}(G)$   
431 we can, in  $\mathbf{L}$ , compute the DFS of such a tree.*

432 **Proof.** For any two cycles  $C_1, C_2$  that are adjacent and any  $v_1 \in C_1, v_2 \in C_2$  it is the  
433 case that there is a directed path in the sublayer from  $v_1$  to  $v_2$  (via  $V(C_1) \cap V(C_2)$ ); thus  
434 inductively the same property holds for any two  $C_1, C_2$  in the same connected component of  
435  $\mathbf{S}^{k+1, l+1}(G)$ . Since  $\mathbf{S}^{k+1, l+1}(G)$  is a planar (undirected) graph, it follows that if it is not a  
436 forest, then it must enclose a facial cycle  $f$ . This facial cycle  $f$  corresponds to a face  $f'$  in  
437 the sublayer  $\mathcal{L}^{k+1, l+1}(\mathbf{Col}(G))$ . Each node on the boundary of  $f$  corresponds to a directed  
438 cycle in  $\mathcal{L}^{k+1, l+1}(\mathbf{Col}(G))$ , and the face  $f'$  must be incident on each of these cycles. By  
439 Lemma 25,  $f'$  must be a red cycle or a blue cycle. Without loss of generality, suppose it  
440 is red. But this means that it cannot intersect a red cycle corresponding to a node on the

441 boundary of  $f$  in more than a vertex. Thus it consists exclusively of edges from some blue  
 442 cycles, call them  $B_1, \dots, B_k$ , on the boundary of  $f$ . Thus  $f'$  is entirely enclosed by the edges  
 443 of  $\cup_{i=1}^k E(B_i) \setminus E(f')$ , which form a blue cycle. This contradicts Lemma 17. ◀

444 Next, we extend the definition of cluster graphs (Definition 19) by contracting the clusters,  
 445 which are maximal trees of the forest  $\mathbf{S}^{k+1, l+1}(G)$  to single vertices:

446 ▶ **Definition 28.** Consider the multigraph  $\mathbf{Cl}^{k+1, l+1}(G)$  on the vertex set  $V(\mathbf{Cl}(G)) = \{v_T : T$   
 447  $\text{is a maximal tree in } \mathbf{S}^{k+1, l+1}(G)\} \cup \{v : v \in V(H) \text{ is colored white in } \mathbf{Col}(G)\}$ ; each edge  
 448 in  $G$  is carried over to  $\mathbf{Cl}^{k+1, l+1}(G)$ , resulting in parallel edges when vertices in  $G$  are merged  
 449 into a single vertex in  $\mathbf{Cl}^{k+1, l+1}(G)$ .

450 Thus, we obtain the following:

451 ▶ **Lemma 29.**  $\mathbf{Cl}^{k+1, l+1}(G)$  is a directed acyclic multigraph for every  $k, l \geq 0$ .

452 **Proof.** Trivial since clusters are the strongly connected components of the sublayer. ◀

## 453 5 The Algorithm for DFS in a Planar Graph

454 Now we will use the layering and lemmas from the previous section to give the final algorithm  
 455 for DFS in a general planar digraph  $H$ , from a root  $r$ . Our output will consist of the edges  
 456 that are included in the DFS tree, along with an ordering on the outgoing tree edges for  
 457 every vertex in the graph, since – in contrast to the case for undirected DFS trees – a  
 458 directed spanning tree may or may not be a DFS tree for different traversals. The ordering  
 459 on outgoing edges for every vertex fixes the traversal.

460 The first step is to build the graph  $G \subseteq H$  consisting of all vertices that are reachable  
 461 from  $r$ , which can be done in  $\mathbf{UL} \cap \mathbf{co-UL}$ . A planar embedding of  $G$  with  $r$  on the external  
 462 face  $f_0$  can then be constructed, using logarithmic space [4, 20].

463 To help make the indexing of our layers simpler, create a “dummy” red cycle (essentially  
 464 just a self loop on a “pseudo-root vertex”  $r'_0$  with an edge from  $r_0$  to  $r$ , where the self loop  
 465 completely encloses  $G$ ; this has the effect of placing the root  $r$  in layer 1.

466 Note that the labeling of  $G$  (described in the previous section) can be computed in  
 467 logspace with an oracle for computing distance in planar graphs. This is because the type of  
 468 each face, edge, and vertex is given by computing distances in the dual graph. Computing  
 469 distance in planar graphs lies in  $\mathbf{UL} \cap \mathbf{co-UL}$  [23, Section 4], and thus computing  $\mathbf{Col}(G)$  can  
 470 be done in  $\mathbf{UL} \cap \mathbf{co-UL}$ .

471 With  $\mathbf{Col}(G)$  in hand, we define a meta tree of the laminar family of colored cycles of  $G$ .

472 ▶ **Definition 30.** For a planar digraph  $G$ , with red and blue cycles given by  $\mathbf{Col}(G)$ , the  
 473 meta tree  $T_G$  is an undirected tree with nodes representing the colored cycles of  $G$ . The  
 474 root node of  $T_G$  is the self-loop on  $r_0$  belonging to sublayer  $\mathcal{L}^{0,1}(\mathbf{Col}(G))$ . For a node in  $T_G$   
 475 representing cycle  $C$  of a sublayer  $\mathcal{L}^{k+1, l+1}(\mathbf{Col}(G))$ , its children are the cycles of the next  
 476 sublayer that are contained inside  $C$ .

477 Note that every node of  $G$  appears in some subgraph  $\mathbf{S}^{k+1, l+1}$  inside some colored cycle  
 478  $C$  of  $\mathbf{Col}(G)$ . First, we describe how to process the subgraph  $C \cup \mathbf{S}^{k+1, l+1}$ , and then we  
 479 describe the order in which we process the colored cycles (which will also determine the  
 480 vertex  $v$  in which we first enter the cycle  $C$ ).

481 Note that the multigraph consisting of  $C$  along with the directed acyclic multigraph  
 482  $\mathbf{Cl}^{k+1, l+1}(G)$  contained in  $C$  is precisely the sort of graph that we showed how to search in

483 Section 3.1. A DFS of this graph can be performed in  $UL \cap \text{co-UL}$ . But many of the nodes of  
 484  $\mathbf{S}^{k+1,l+1}$  are not simply nodes of  $G$ , but are clusters of cycles in  $G$ . Thus we must output a  
 485 DFS not of  $\mathbf{CI}^{k+1,l+1}(G)$  but a DFS of the corresponding nodes in  $G$ .

- 486 1. Start the DFS of  $C \cup$  the multigraph  $\mathbf{CI}^{k+1,l+1}(G)$  that lies within  $C$ , as described in  
 487 Section 3.1, by following the edges of  $C$  until we come back to the entry vertex  $v$ .
- 488 2. Then start backtracking along  $C$  and performing a DFS of the directed acyclic multigraph  
 489  $\mathbf{CI}^{k+1,l+1}(G)$ . Each time we follow an edge to a new vertex  $D$  of  $\mathbf{CI}^{k+1,l+1}(G)$  that  
 490 represents a cluster of  $G$ , this edge corresponds to an edge  $e$  of  $G$  to a node  $x$  on one of  
 491 the cycles of the undirected tree of cycles that constitutes the cluster  $D$ . The ordering  
 492 of the neighbors of  $D$  (that is used in constructing the lexicographic-least DFS tree  
 493 of  $\mathbf{CI}^{k+1,l+1}(G)$ ) consists of the order in which edges out of  $D$  are encountered while  
 494 searching the tree of cycles that constitutes  $D$ , when starting at vertex  $x$ ; this ordering  
 495 can be computed in logspace.
- 496 3. Each vertex of  $D$  of  $\mathbf{CI}^{k+1,l+1}(G)$  represents a tree of cycles. Each cycle in the cluster is  
 497 explored by going from its entry vertex directly around the cycle, and then backtracking  
 498 to explore its neighbor cycles in the cluster. This is easy to perform in logspace. (This  
 499 sequence of exploring the cycles in  $D$  imposes the order on the edges that leave  $D$  to other  
 500 clusters in  $\mathbf{CI}^{k+1,l+1}(G)$ , which gives us the ordering that determines the lexicographically-  
 501 least DFS tree of  $\mathbf{CI}^{k+1,l+1}(G)$ .)
- 502 4. The lexicographically-least DFS tree of  $\mathbf{CI}^{k+1,l+1}(G)$  identifies the edge that should be  
 503 used to visit each neighbor of  $D$ . Explore each vertex of  $\mathbf{CI}^{k+1,l+1}(G)$  in turn in this way.

504 And now we describe the algorithm that determines the order in which we process the  
 505 colored cycles. For each node  $C$  in the meta tree  $T_G$ , (and recall that each node in  $T_G$   
 506 corresponds to a colored cycle), find the unique path in  $T_G$  from the root to  $C$ . Then start  
 507 following that path; for each edge  $C_1 \rightarrow C_2$  in that path, we start by knowing the vertex  $v$   
 508 in  $C_1$  where the tree constructed thus far entered  $C_1$ . (Initially,  $C$  is the self loop on  $r_0$ , and  
 509  $v = r_0$ .)

510 Follow the procedure outlined above for processing the DFS tree inside of  $C_1$ , but do not  
 511 produce any output. Instead, wait for the moment when  $C_2$  is encountered in that process.  
 512 (It will be encountered, because otherwise there would not be an edge  $C_1 \rightarrow C_2$  in the meta  
 513 tree.) At that point, remember the vertex  $x$  where cycle  $C_2$  is first entered, and then start  
 514 processing the next edge in the path from the root to  $C$ .

515 When  $C$  is finally reached, we remember the vertex where  $C$  was entered, and start  
 516 outputting the DFS tree for the subgraph inside  $C$ , as above.

517 We must also give the orderings of outgoing tree edges around every vertex. For a white  
 518 vertex of any sublayer, the outgoing edges belong to the same sublayer and their ordering is  
 519 already defined by the algorithm in section 3.1. For the other case, we analyze:

520 Suppose  $v$  is a vertex on a colored cycle  $C$  of some sublayer. Let the outgoing tree edges  
 521 be  $e, e'_1, e'_2 \dots e'_k, e''_1, e''_2 \dots e''_l$ , where  $e$  is the outgoing edge that belongs to cycle  $C$ ,  $e'_1, e'_2 \dots e'_k$   
 522 are the outgoing edges other than  $e$  that belong to the same layer as  $v$  (they consist of edges  
 523 going out of  $C$ , either white edges going out from the cluster or colored edges of the same  
 524 cluster), and  $e''_1, e''_2 \dots e''_l$  are the outgoing edges of the *next* layer (edges going inside of  $C$ ).

525 Then the order of these edges for DFS is:

- 526 ■ First we take the white edges among  $e'_1 \dots e'_k$ .
- 527 ■ Then we take  $e$  (finish the cycle).
- 528 ■ Then we take the colored outgoing edges among  $e'_1 \dots e'_k$ .
- 529 ■ Then we take the edges of the next layer,  $e''_1 \dots e''_l$ .

530 The order of edges *within* each of these steps is already defined in section 3.1 or in steps  
 531 2 and 3 of the algorithm above. This gives an ordering of all outgoing tree edges for any  
 532 vertex  $v$ .

533 We could interchange between last two points of the ordering, and still the algorithm  
 534 would give DFS trees albeit different ones. However it is crucial that  $e$  is taken before  $e_1'' \dots e_l''$   
 535 for all vertices, i.e. we finish the cycle before going inside to higher sublayers.

536 The algorithm clearly can be implemented in logspace with an oracle for  $UL \cap \text{co-}UL$ , and  
 537 it clearly outputs a tree that spans  $G$ .

538 Now we must show that the tree that is produced is a DFS tree.

539 Our algorithm definitely produces a spanning tree of the set of all vertices in  $G$  that are  
 540 reachable from the start vertex  $r$ . In order to show that the tree is a DFS tree, it suffices to  
 541 show that, for any edge  $(u, v)$  of  $G$  that is not in the tree, in our depth-first traversal of the  
 542 tree the vertex  $v$  is visited before  $u$ , or else  $v$  is visited from a descendent of  $u$  in the tree.

543 Either  $u$  and  $v$  are in the same level, or else  $u$  and  $v$  are at different levels.

544 ■ Case 1:  $u$  and  $v$  are in the same sublayer:

545 Then either  $u$  and  $v$  are in the same cluster, or they are not. If they are not in the same  
 546 cluster, then the cluster that  $v$  is in is visited by some lexicographically-earlier edge from  
 547 the cluster in which  $u$  resides. Thus  $v$  is visited before  $u$  in the depth-first traversal of  
 548 the tree.

549 If  $u$  and  $v$  are in the same cluster, then either they are in the same colored cycle, or they are  
 550 not. If they are in the same colored cycle, and the edge  $(u, v)$  is not in the tree, it can  
 551 either be because  $v$  is the first vertex visited in the cycle, and thus  $v$  is visited before  $u$ ,  
 552 or else edge  $(u, v)$  is a chord of the cycle containing  $u, v$  (but the chord itself is in the  
 553 next sublayer by definition). Since we traverse the cycle first and then branch inside,  
 554 edge  $(u, v)$  is either a forward edge or a back edge depending on whether  $u$  comes first in  
 555 cycle or  $v$ .

556 If  $u$  and  $v$  are in different colored cycles in the same cluster, then there is not an edge  
 557  $(u, v)$ .

558 ■ Case 2:  $v$  is in a higher sublayer than  $u$

559 In this case  $u$  must be on a colored cycle  $C$  and  $v$  lies inside  $C$ , in the next sublayer.  
 560 Since in our algorithm we complete the traversal of cycle  $C$  first and then explore the  
 561 clusters inside, the only way  $(u, v)$  can be a non tree edge is when  $v$  has been explored in  
 562 the subtree of a vertex  $u'$  that occurs after  $u$  in traversal of  $C$ , while backtracking. The  
 563 edge  $(u, v)$  is therefore a forward edge.

564 ■ Case 3:  $u$  is in a higher sublayer than  $v$

565 This case is similar to previous one and the same argument shows that  $v$  must be on a  
 566 colored cycle and the edge  $(u, v)$  is a back edge.

567 Thus our tree is a DFS tree.

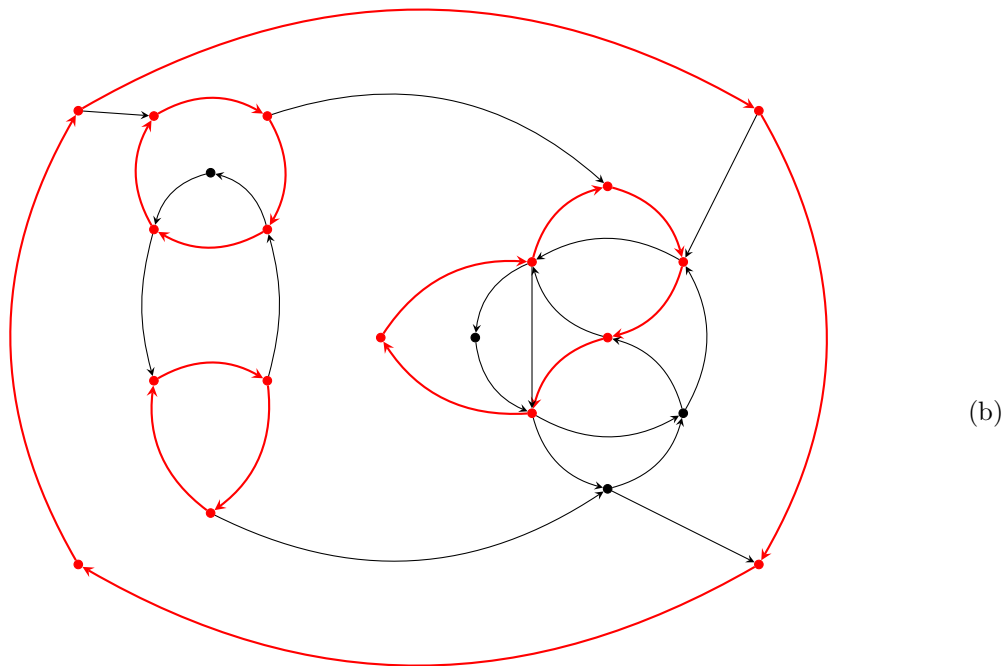
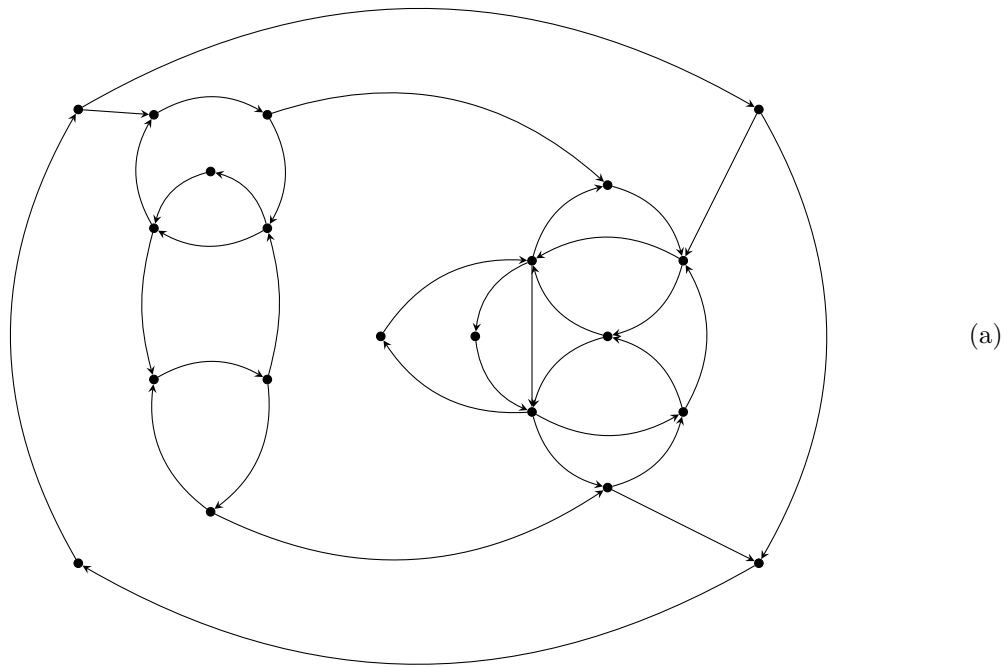
## 568 ——— References ———

- 569 1 Alok Aggarwal, Richard J. Anderson, and Ming-Yang Kao. Parallel depth-first search in  
 570 general directed graphs. *SIAM J. Comput.*, 19(2):397–409, 1990. doi:10.1137/0219025.
- 571 2 Eric Allender, David A. Mix Barrington, Tanmoy Chakraborty, Samir Datta, and Sambuddha  
 572 Roy. Planar and grid graph reachability problems. *Theory of Computing Systems*, 45(4):675–  
 573 723, 2009. doi:10.1007/s00224-009-9172-z.
- 574 3 Eric Allender, Archit Chauhan, Samir Datta, and Anish Mukherjee. Planarity, exclusivity,  
 575 and unambiguity. *Electronic Colloquium on Computational Complexity (ECCC)*, 26:39, 2019.

- 576 4 Eric Allender and Meena Mahajan. The complexity of planarity testing. *Inf. Comput.*,  
577 189:117–134, 2004.
- 578 5 Eric Allender, Klaus Reinhardt, and Shiyu Zhou. Isolation, matching, and counting: Uniform  
579 and nonuniform upper bounds. *Journal of Computer and System Sciences*, 59(2):164–181,  
580 1999.
- 581 6 Sanjeev Arora and Boaz Barak. *Computational Complexity, a modern approach*. Cambridge  
582 University Press, 2009.
- 583 7 Tetsuo Asano, Taisuke Izumi, Masashi Kiyomi, Matsuo Konagaya, Hirotaka Ono, Yota Otachi,  
584 Pascal Schweitzer, Jun Tarui, and Ryuhei Uehara. Depth-first search using  $O(n)$  bits. In  
585 Hee-Kap Ahn and Chan-Su Shin, editors, *Proc. 25th International Symposium on Algorithms  
586 and Computation (ISAAC)*, volume 8889 of *Lecture Notes in Computer Science*, pages 553–564.  
587 Springer, 2014. doi:10.1007/978-3-319-13075-0\_44.
- 588 8 Chris Bourke, Raghunath Tewari, and N. V. Vinodchandran. Directed planar reachability is  
589 in unambiguous log-space. *TOCT*, 1(1):4:1–4:17, 2009. URL: [http://doi.acm.org/10.1145/  
590 1490270.1490274](http://doi.acm.org/10.1145/1490270.1490274), doi:10.1145/1490270.1490274.
- 591 9 Pilar de la Torre and Clyde P. Kruskal. Fast parallel algorithms for all-sources lexicographic  
592 search and path-algebra problems. *J. Algorithms*, 19(1):1–24, 1995. doi:10.1006/jagm.1995.  
593 1025.
- 594 10 Pilar de la Torre and Clyde P. Kruskal. Polynomially improved efficiency for fast parallel  
595 single-source lexicographic depth-first search, breadth-first search, and topological-first search.  
596 *Theory Comput. Syst.*, 34(4):275–298, 2001. doi:10.1007/s00224-001-1008-4.
- 597 11 Reinhard Diestel. *Graph Theory*, volume 173 of *Graduate texts in mathematics*. Springer,  
598 2016.
- 599 12 Amr Elmasry, Torben Hagerup, and Frank Kammer. Space-efficient basic graph algorithms.  
600 In *Proc. 32nd International Symposium on Theoretical Aspects of Computer Science (STACS)*,  
601 volume 30 of *LIPICs*, pages 288–301. Schloss Dagstuhl - Leibniz-Zentrum für Informatik, 2015.  
602 doi:10.4230/LIPICs.STACS.2015.288.
- 603 13 Torben Hagerup. Planar depth-first search in  $O(\log n)$  parallel time. *SIAM J. Com-*  
604 *put.*, 19(4):678–704, June 1990. URL: <http://dx.doi.org/10.1137/0219047>, doi:10.1137/  
605 0219047.
- 606 14 Torben Hagerup. Space-efficient DFS and applications to connectivity problems: Simpler,  
607 leaner, faster. *Algorithmica*, 82(4):1033–1056, 2020. doi:10.1007/s00453-019-00629-x.
- 608 15 Taisuke Izumi and Yota Otachi. Sublinear-space lexicographic depth-first search for bounded  
609 treewidth graphs and planar graphs. In *Proc. 47th International Colloquium on Automata, Lan-*  
610 *guages and Programming (ICALP)*, *LIPICs*. Schloss Dagstuhl - Leibniz-Zentrum für Informatik,  
611 2020. to appear.
- 612 16 B. Jenner and B. Kirsig. *Alternierung und Logarithmischer Platz*. Dissertation, Universität  
613 Hamburg, 1989.
- 614 17 Ming-Yang Kao and Philip N. Klein. Towards overcoming the transitive-closure bottleneck:  
615 Efficient parallel algorithms for planar digraphs. *Journal of Computer and System Sciences*,  
616 47(3):459–500, 1993. doi:10.1016/0022-0000(93)90042-U.
- 617 18 Maxim Naumov, Alysson Vrieling, and Michael Garland. Parallel depth-first search for directed  
618 acyclic graphs. In *Proc. 7th Workshop on Irregular Applications: Architectures and Algorithms*,  
619 pages 4:1–4:8, 2017. doi:10.1145/3149704.3149764.
- 620 19 John H. Reif. Depth-first search is inherently sequential. *Inf. Process. Lett.*, 20(5):229–234,  
621 1985. doi:10.1016/0020-0190(85)90024-9.
- 622 20 Omer Reingold. Undirected connectivity in log-space. *J. ACM*, 55(4), 2008.
- 623 21 Klaus Reinhardt and Eric Allender. Making nondeterminism unambiguous. *SIAM J. Comput.*,  
624 29(4):1118–1131, 2000. URL: <https://doi.org/10.1137/S0097539798339041>, doi:10.1137/  
625 S0097539798339041.

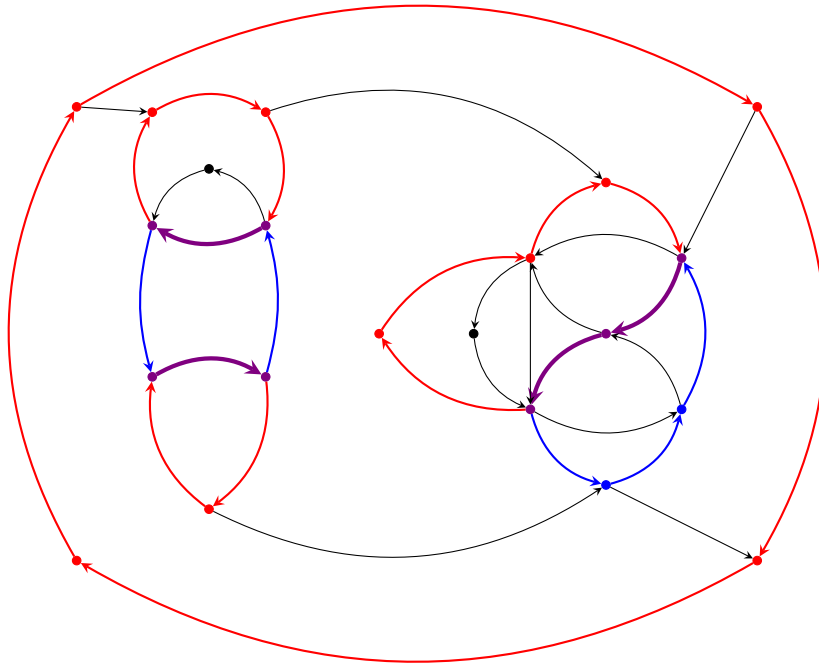
- 626 22 Raghunath Tewari and N. V. Vinodchandran. Green's theorem and isolation in planar  
627 graphs. *Inf. Comput.*, 215:1–7, 2012. URL: <https://doi.org/10.1016/j.ic.2012.03.002>,  
628 doi:10.1016/j.ic.2012.03.002.
- 629 23 Thomas Thierauf and Fabian Wagner. The isomorphism problem for planar 3-connected  
630 graphs is in unambiguous logspace. *Theory Comput. Syst.*, 47(3):655–673, 2010. doi:10.1007/  
631 s00224-009-9188-4.
- 632 24 H. Vollmer. *Introduction to Circuit Complexity: A Uniform Approach*. Springer-Verlag New  
633 York Inc., 1999. doi:10.1007/978-3-662-03927-4.



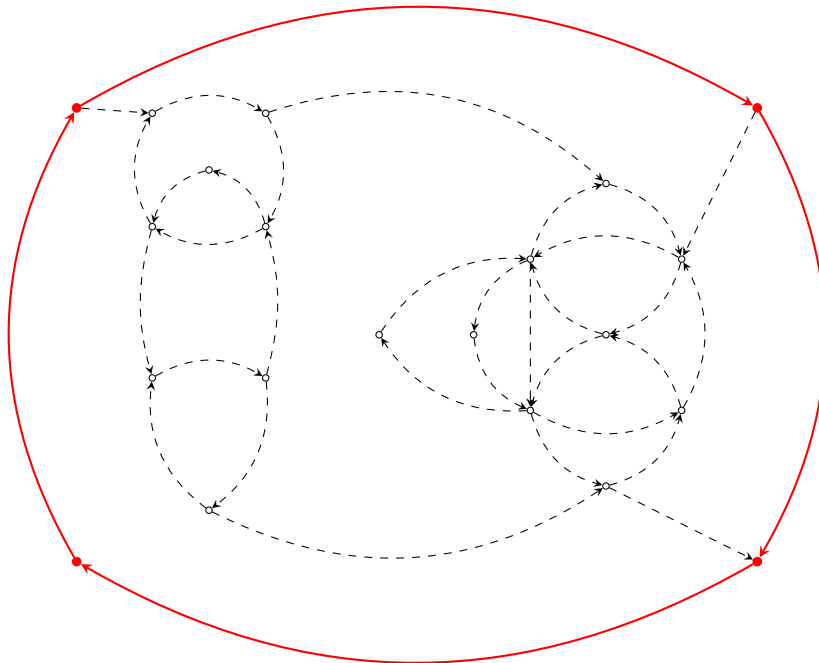


■ **Figure 2** Figure (a) is a graph  $G$ . Figure (b) is the graph in (a) after labelling red edges using clockwise dual. We omit the cycle expansion and contraction procedure here.

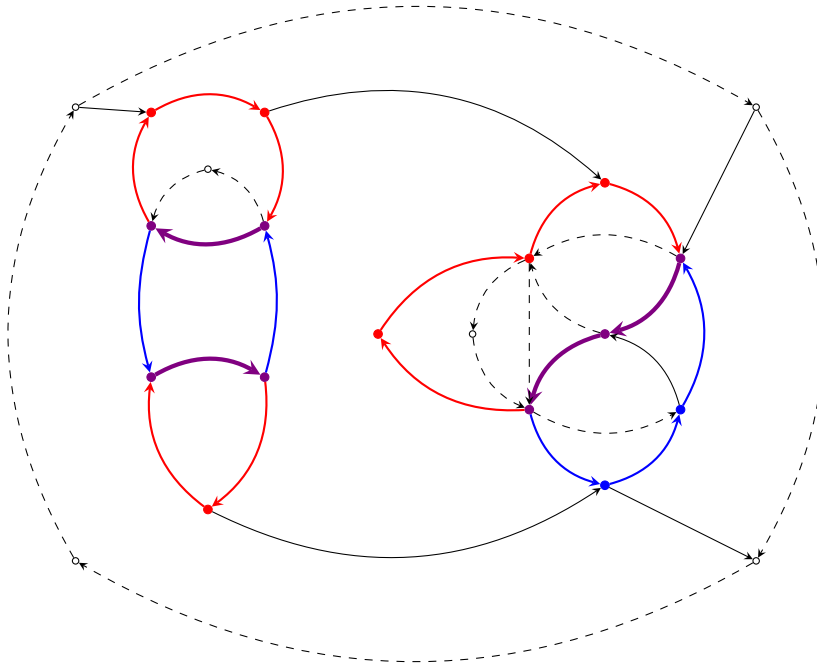




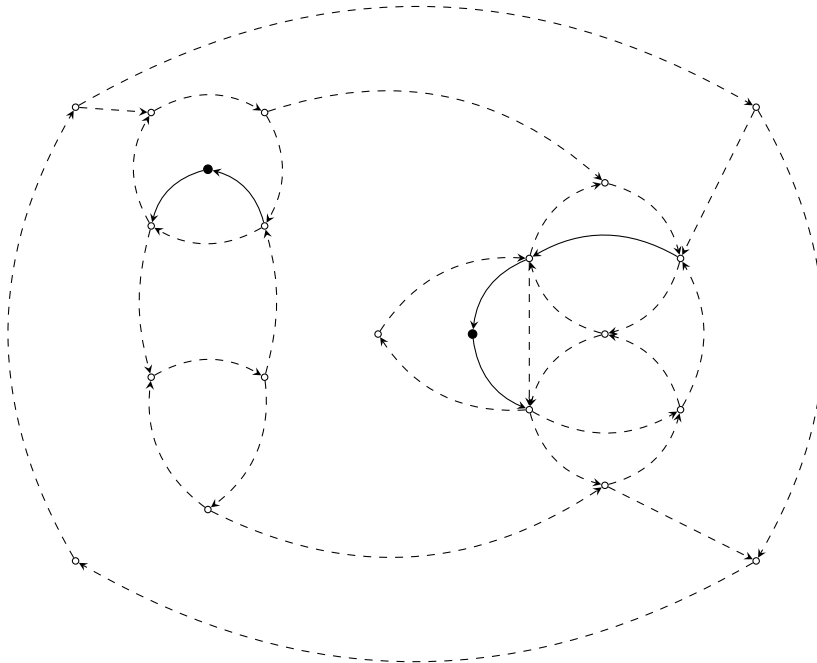
■ **Figure 3** This figure shows  $G$  after applying blue labellings to each red layer we obtained in the previous figure. The vertices and edges colored purple are those that are red as well as blue.



■ **Figure 4** This figure represents the sublayer  $(1, 1)$ . The dashed edges and empty vertices are not part of the layer.



■ **Figure 5** This figure represents the sublayer (2, 1).



■ **Figure 6** This figure represents the sublayer (3, 1)